

Supplement to “Improving Ice Sheet Model Calibration Using Paleo and Modern-observations: A Reduced Dimensional Approach”

Won Chang, Murali Haran, Patrick Applegate, and David Pollard

May 3, 2016

S1 Modern binary patterns from PSU3D-ICE model

Figure S1 shows some example modern binary patterns from our PSU3D-ICE model runs. As seen in the lower right (upper left) “outer” blocks of this figure, larger (smaller) OCFAC and CALV values both cause more (less) ice wastage and grounding-line retreat. These parameters control the strength of oceanic sub-ice melting and calving, respectively, and dominate variations of the other two parameters, CRH and TAU. Within each outer block, the 9 inner panels show the effects of CRH and TAU. Larger CRH (bed sliding coefficient) results in thinner grounded ice and more retreat, and larger TAU (time scale of bed rebound) results in deeper grounding lines and more retreat. However these effects are relatively minor compared to those in the outer blocks produced by OCFAC and CALV.

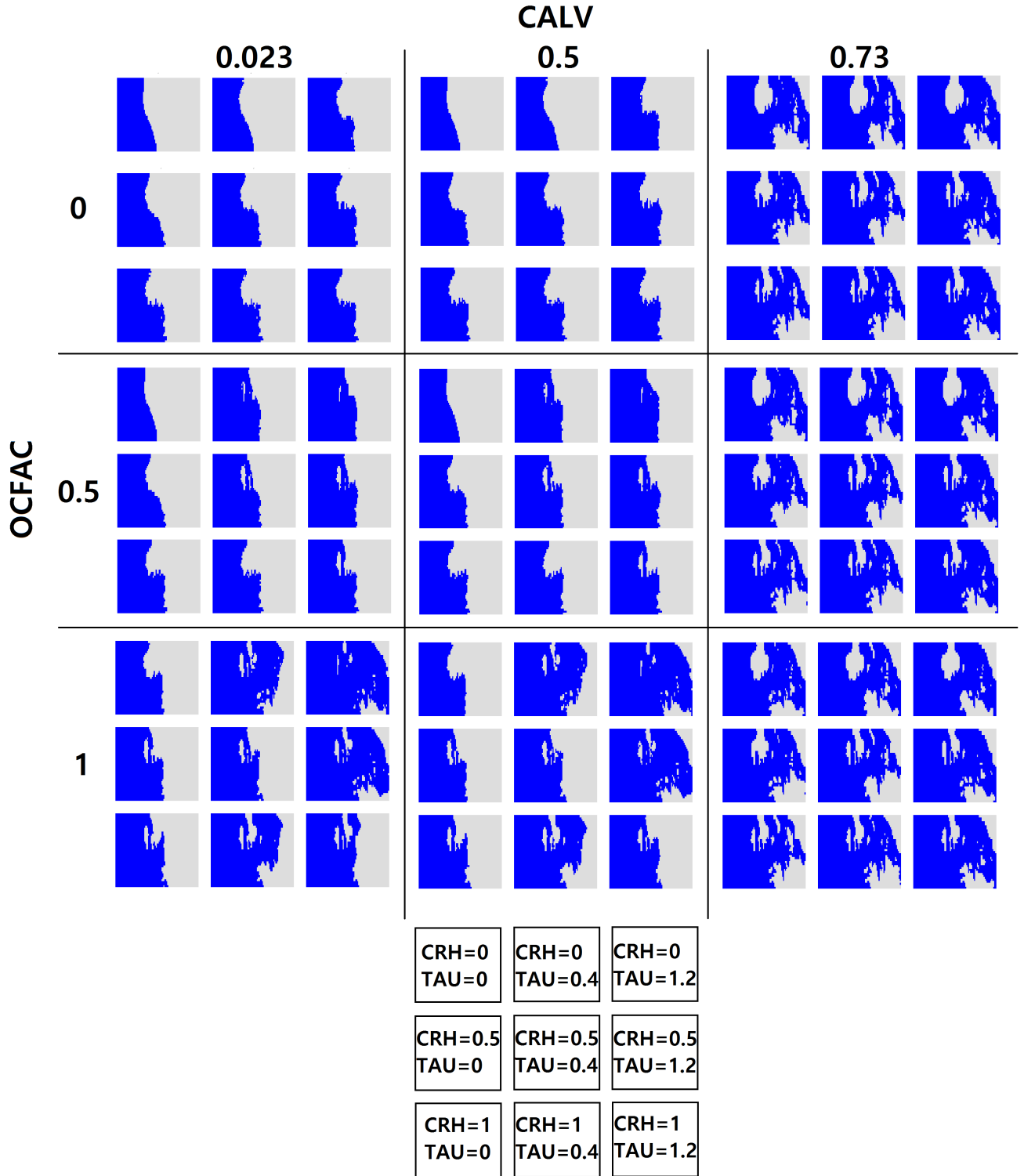


Figure S1: Example modern binary patterns from the model outputs at various input parameter settings. The values on the left and upper edges show the parameter settings for OCFAC and CALV respectively. The bottom-most panel shows the configuration of the values of CRH and TAU for each panel.

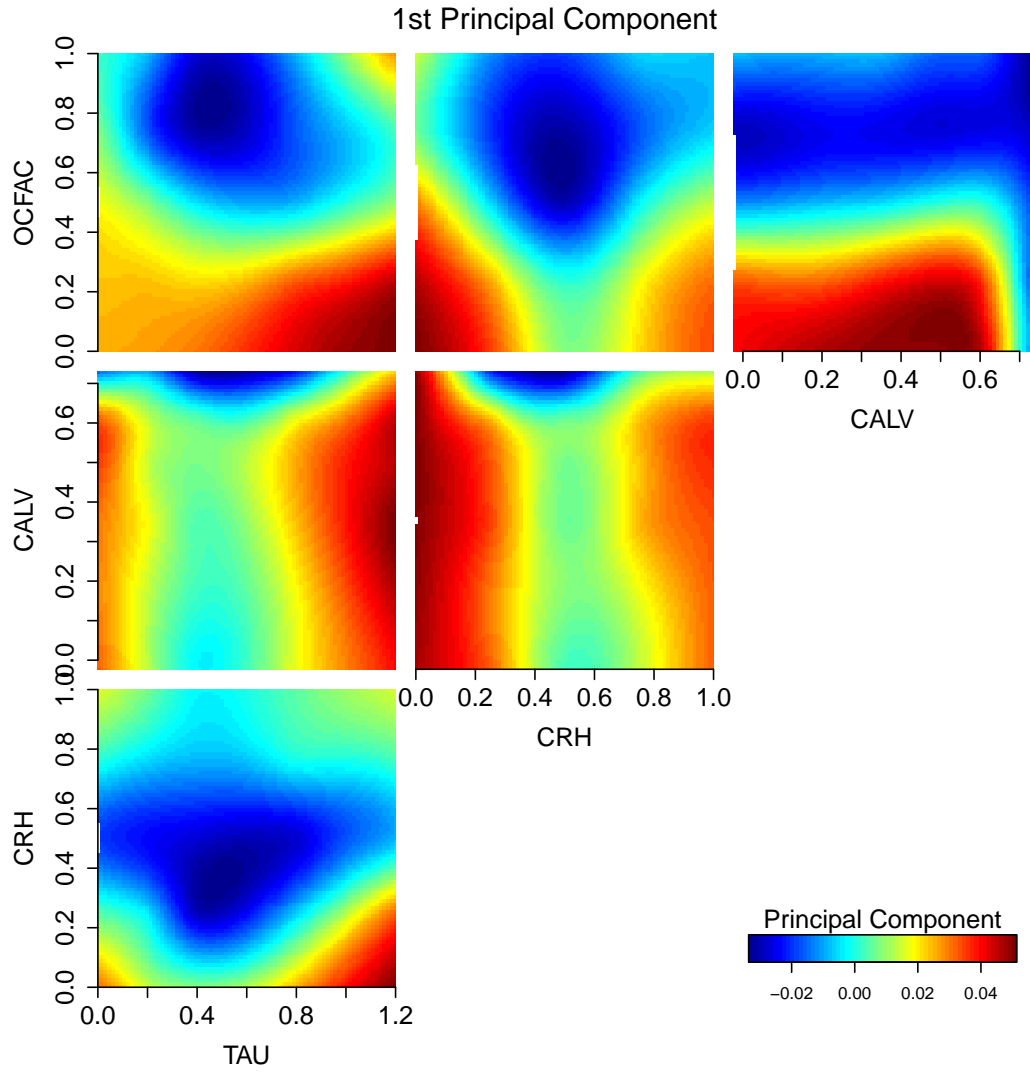


Figure S2: The values of the first logistic principal component for modern binary patterns at different input parameter settings.

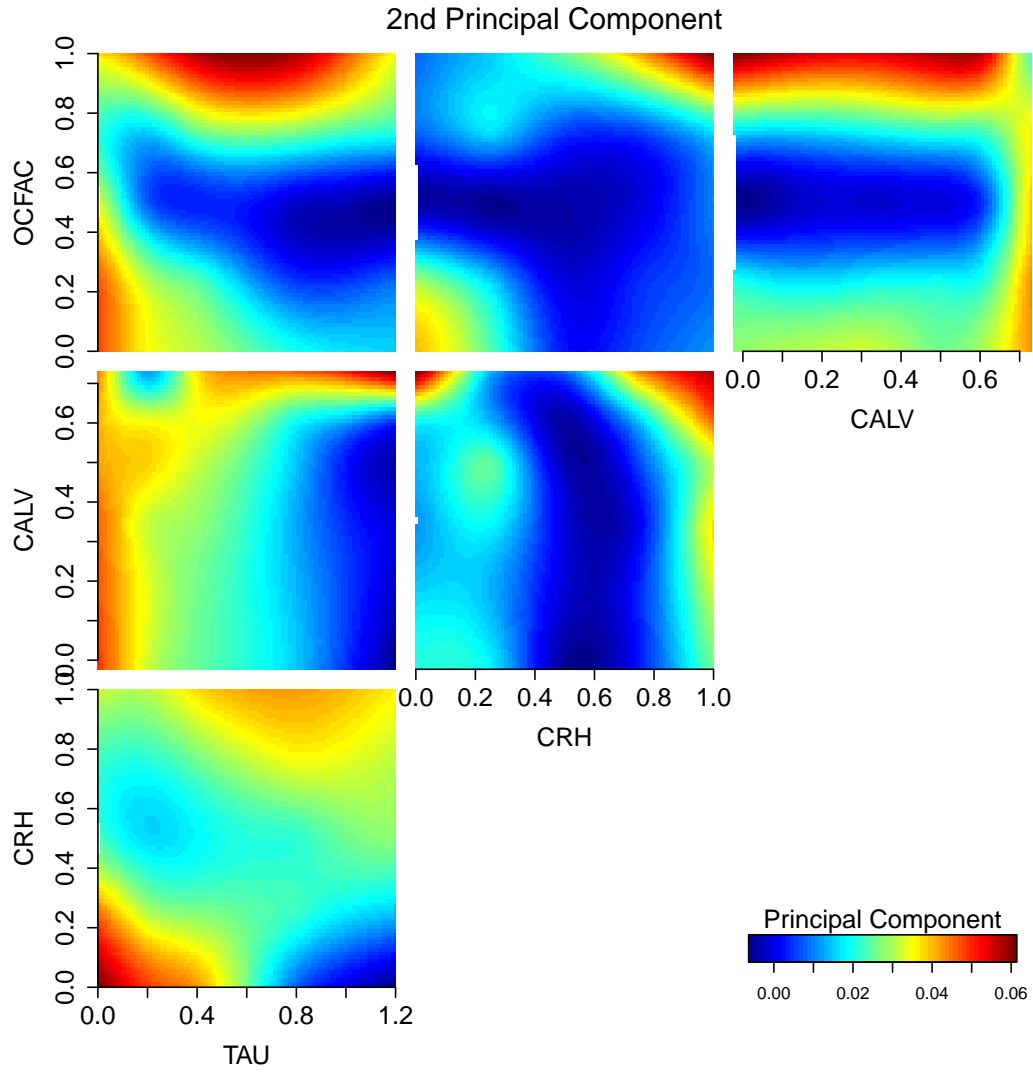


Figure S3: The values of the second logistic principal component for modern binary patterns at different input parameter settings.

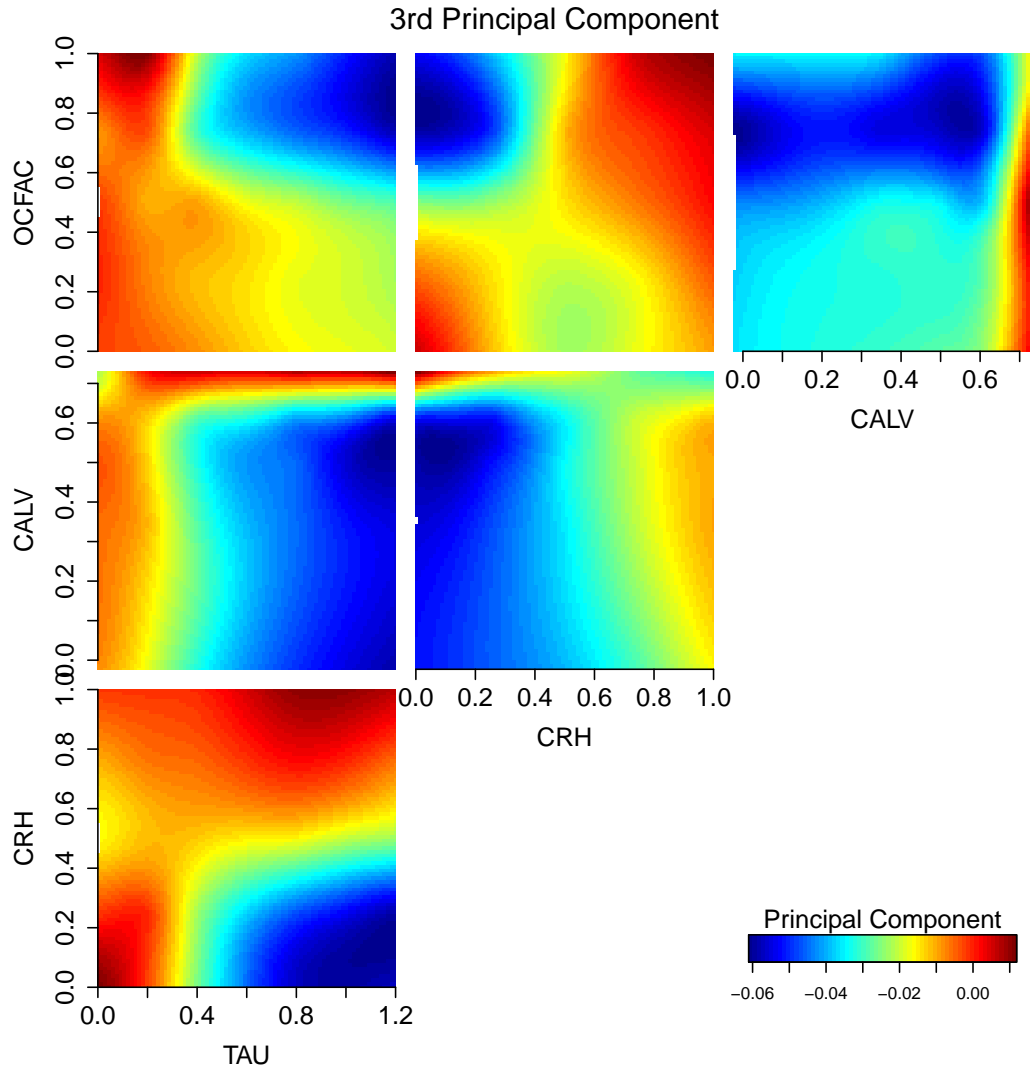


Figure S4: The values of the third logistic principal component for modern binary patterns at different input parameter settings.

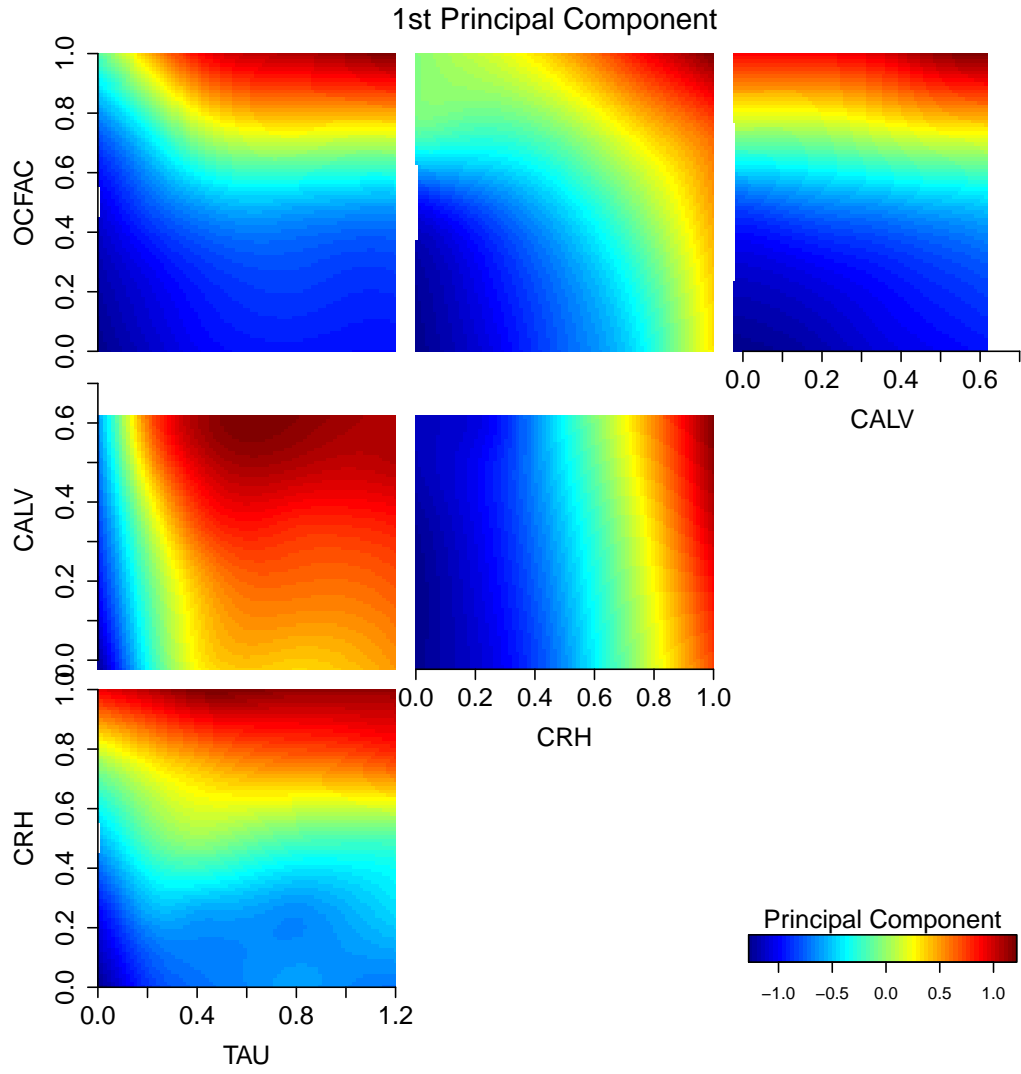


Figure S5: The values of the first principal component for past grounding line positions at different input parameter settings.

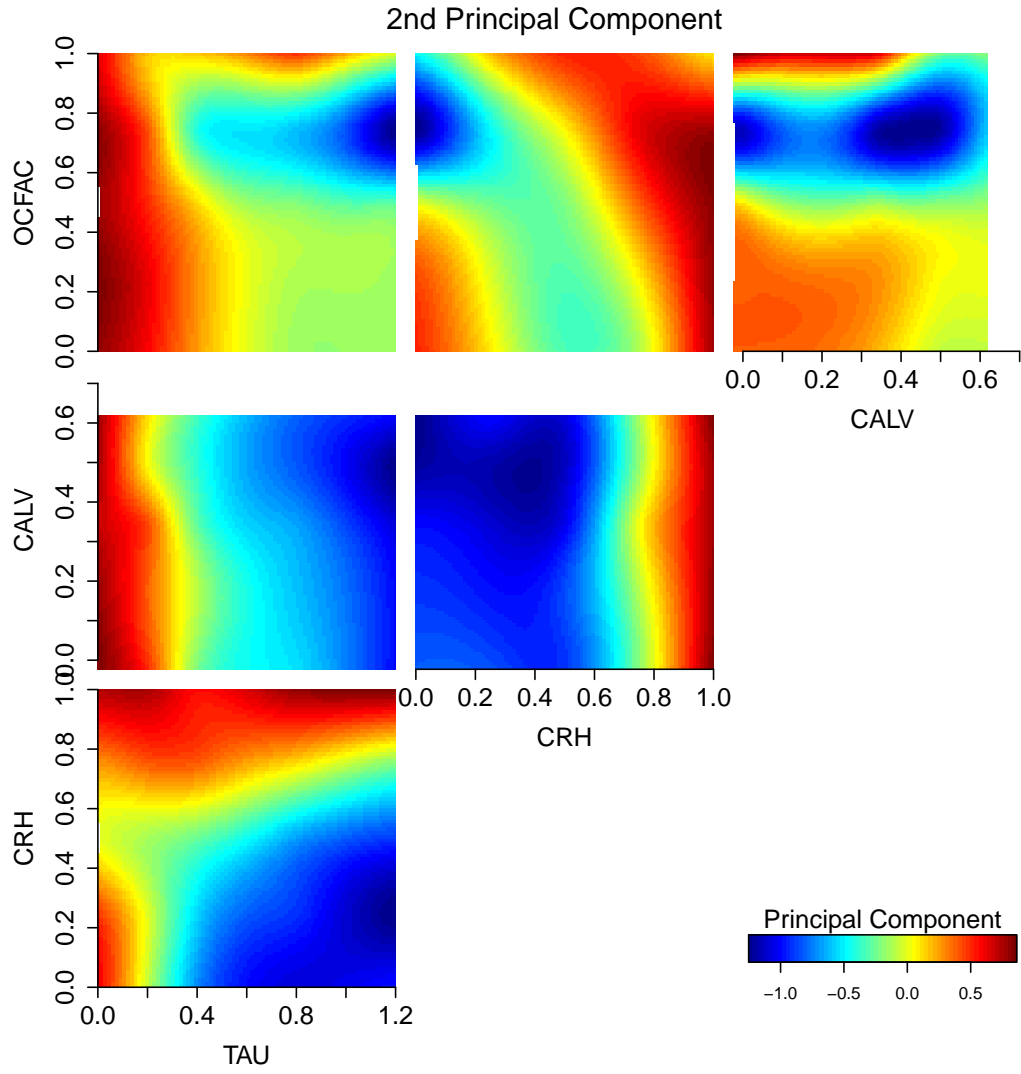


Figure S6: The values of the second principal component for past grounding line positions at different input parameter settings.

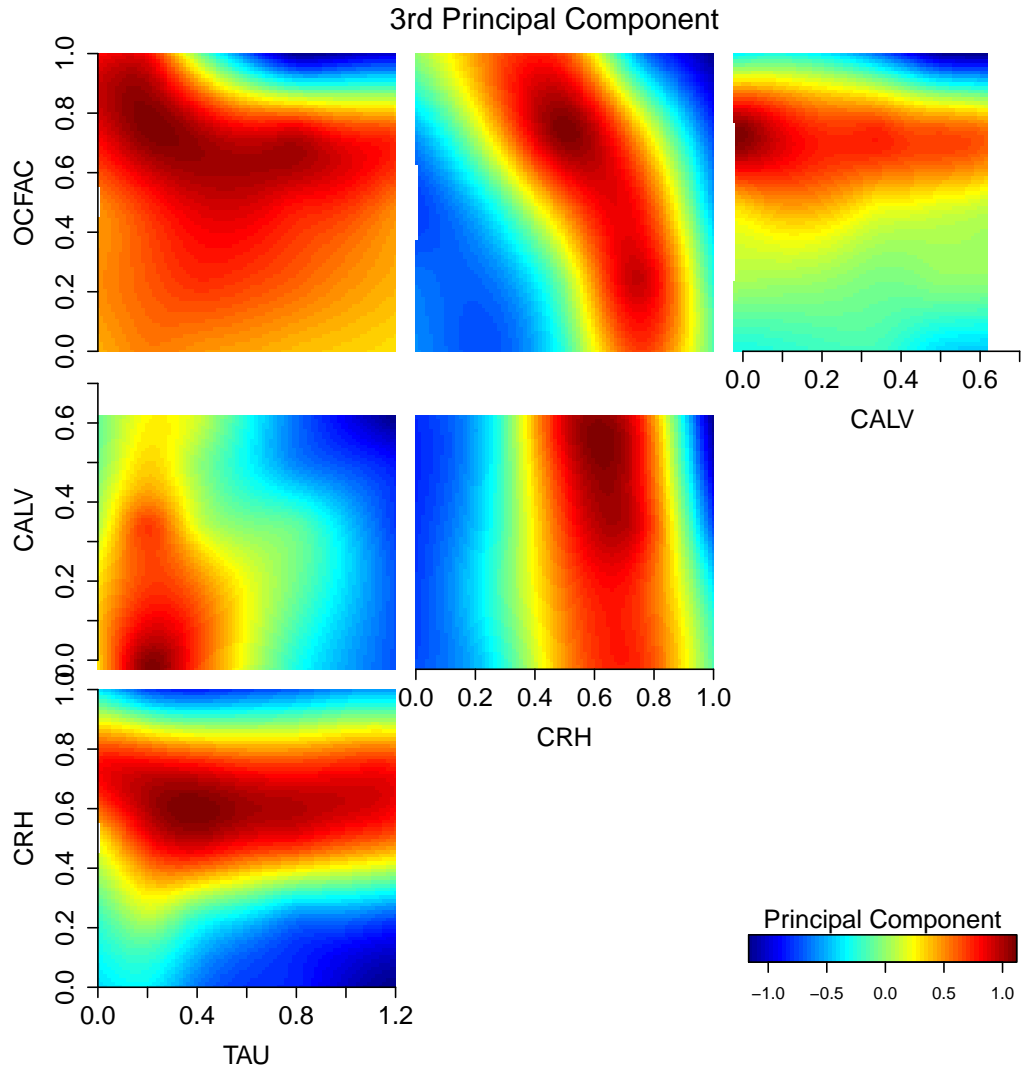


Figure S7: The values of the third principal component for past grounding line positions at different input parameter settings.

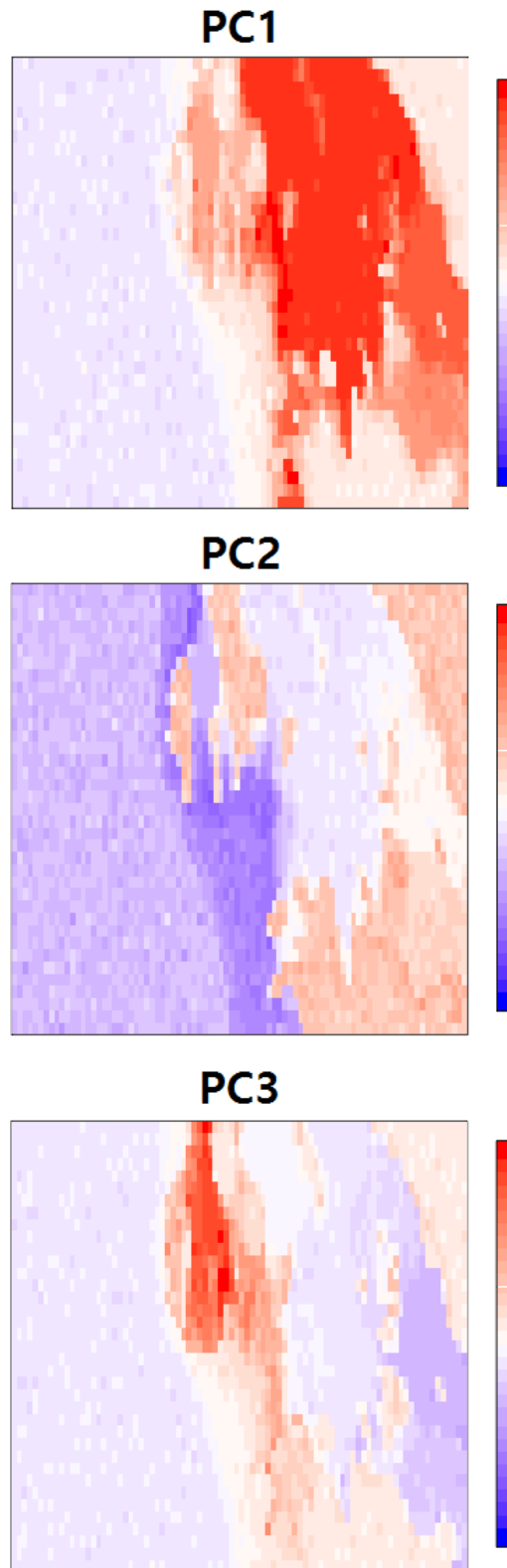


Figure S8: The three leading logistic principal components for modern binary patterns.

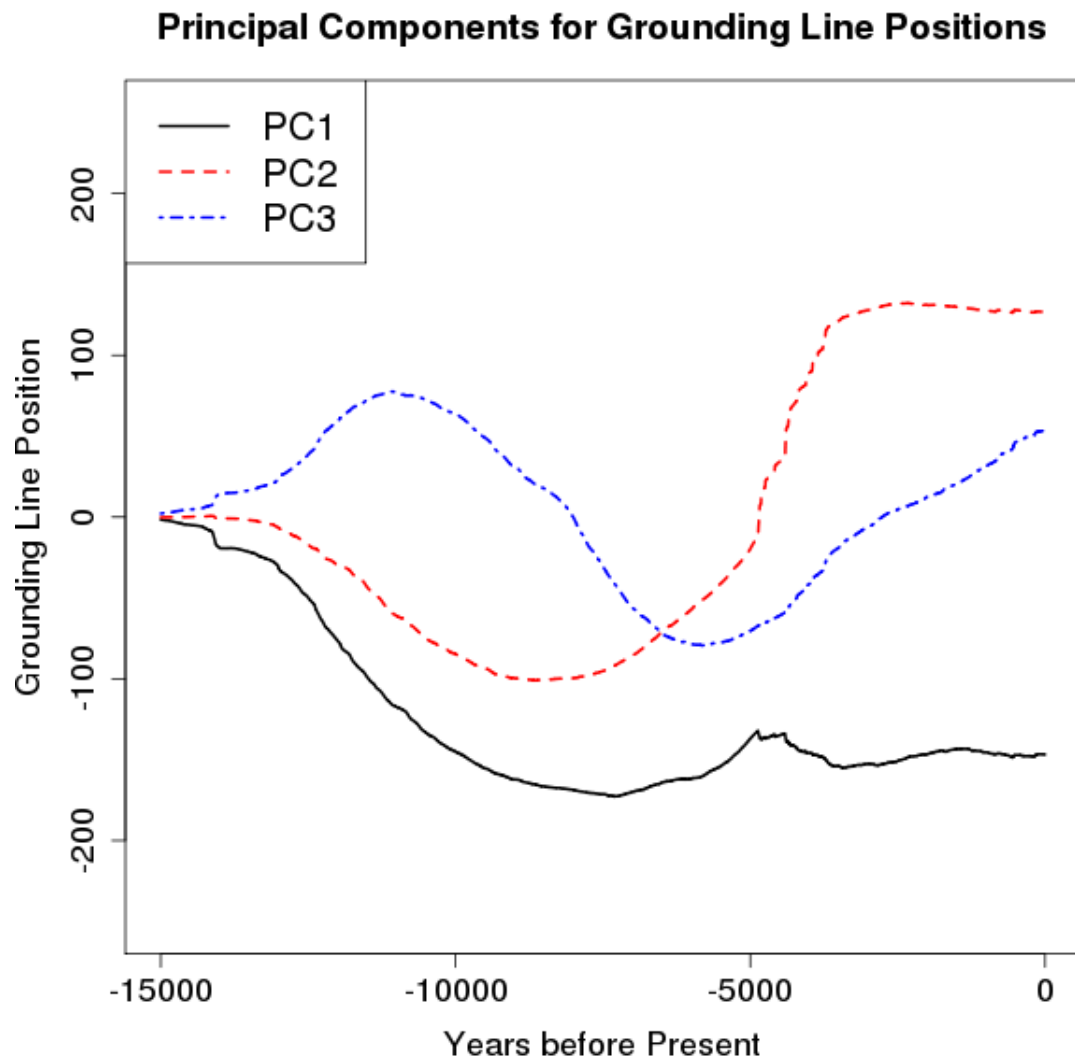


Figure S9: The three leading principal components for past grounding line positions.